Wear 301 (2013) 192–200

Contents lists available at SciVerse ScienceDirect

Wear

journal homepage: www.elsevier.com/locate/wear

Predicting the wear of hard-on-hard hip joint prostheses

M.S. Uddin, L.C. Zhang*

School of Mechanical and Manufacturing Engineering, The University of New South Wales, NSW 2052, Australia

ARTICLE INFO

Article history:
Received 22 August 2012
Received in revised form
4 January 2013
Accepted 7 January 2013
Available online 16 January 2013

Keywords:
Hip joint prostheses
3D FE simulation
Contact stress
Wear

ABSTRACT

The wear of the bearing surfaces of hip joint prostheses is a key problem causing their primary failure. This paper introduces a wear prediction model with the aid of the finite element analysis. To mimic walking, the most common activity of a human body, a three-dimensional physiological loading gait cycle was considered. The wear at the bearing surface in gait cycles was calculated based on the contact stress variation from the finite element analysis and the sliding distance obtained from three-dimensional hip gait motions. The geometry of the worn surface was updated considering the average routine activities of a patient. The model was applied to three hard-on-hard prostheses, i.e., PCD (polycrystalline diamond)-on-PCD, ceramic-on-ceramic and metal-on-metal couples. It was found that due to the gait motion, the intensity and location of the maximum contact stress in the bearing components change with the gait instances. With a given geometry and gait loading, the linear and volumetric wear on the cup surface increases with the number of gait cycles. With increasing the gait cycles, the surface wear can bring about scattered contact pressure distribution. Compared to the ceramic-on-ceramic and metal-on-metal couples, the PCD-on-PCD bearing has the lowest wear progression. It was also concluded that the computational wear model presented in this paper can reasonably predict the wear evolution in hard-on-hard hip implants.

1. Introduction

Total hip replacement (THR) is one of the most successful applications of biomaterials in the medical industry. In THR, a spherical head connected to the femoral stem articulates against a spherical cup/liner attached to the pelvic bone. Substantial research on hip prostheses has been carried out to understand and evaluate their preclinical and clinical performance in terms of contact stresses, friction and wear, and mechanical reliability [1,2]. It has been shown that contact stresses in the bearing surfaces is critical to the progress of wear and hence affecting significantly the life of hip prostheses. In daily routine activities, a hip joint undergoes three-dimensional (3D) motions and gait loads, and its bearing surfaces always experience varying contact stresses. Such repeated operation with time causes wear and damage of the bearing surfaces, and as a result, leads to osteolysis and aseptic loosening [3,4].

Conventionally, hard-on-soft bearing couples such as metal-on-UHMWPE (ultrahigh molecular weight polyethylene) and ceramic-on-UHMWPE were widely used in THR. However, the wear debris released from the soft UHMWPE degrades the life of the hip implants. Recently, new materials of high wear resistance have been available and advanced surface finish and lubrication techniques have been developed. Hence, hard-on-hard bearing couples, such as metal-on-metal and ceramic-on-ceramic, have been extensively used to reduce wear debris generation and hence to improve the performance of the hip joint prostheses. However, there are still many vital problems such as osteolysis due to the metal ion released from metallic wear debris and due to the fracture of ceramics caused by the unexpected edge loading. To overcome these difficulties, PCD has been proposed as a potential bearing material for hip joint prostheses due to its excellent mechanical properties (e.g., high strength, toughness, ultra-low friction) and superior biocompatibility [5,6]. This PCD is manufactured by small diamond grains under a high temperature and high pressure sintering environment.

As an important performance index of hip joint prostheses, wear progression of the bearing surfaces must be understood accurately. Previously both clinical and laboratory studies attempted to measure the wear of the implants to assess their performance [7,9]. For instances, Essner et al. [8] carried out hip simulator tests using a simplified loading cycle, and compared and statistically analyzed the wear on ceramic-on-PE, metal-on-metal and ceramic-on-ceramic hip joint prostheses for a short period of time up to 5 million cycles. Such *in-vitro* tests are usually time-consuming and costly, which is especially the case when a comprehensive understanding on the roles of many design parameters is needed.

The finite element method (FEM) as a powerful computational tool has been widely used to improve the design of hip joint prostheses and to minimise the expensive experimental trials. Many investigations have been conducted, using the FEM, to

* Corresponding author. Tel.: +61 2 93856078; fax: +61 2 9385 7316.
E-mail address: Liangchi.Zhang@unsw.edu.au (L.C. Zhang).

0043-1648/$ - see front matter © 2013 Elsevier B.V. All rights reserved.
http://dx.doi.org/10.1016/j.wear.2013.01.009

understand the contact stresses, deformation, damage and failure of the prostheses [10,11]. Using *in-vivo* loads for the stance phase of the gait cycle and simplified kinematics of the joint, Maxian et al. [12] simulated the wear of soft UHMWPE cup and the damage layout. Teoh et al. [13] extended the Maxian's model and conducted a parametric wear simulation of UHMWPE liner surfaces by considering the elasto-plastic properties of the material. By incorporating the creep deformation using the material's uniaxial creep law, Bevil et al. [14] simulated the effect of some design parameters such as head size, radial clearance, and liner thickness on the volumetric wear and penetration depth of a soft UHMWPE liner surface. Matsoukas et al. [15] and Kang et al. [16] carried out a 3D finite element analysis by incorporating both creep and cross-shear principles. Most computational wear analysis mentioned above focused on the wear on soft acetabular liner surfaces which articulate against a femoral head. For the ease of computational modelling, they sometimes used very simplified hip kinematic and gait load, such as one-dimensional vertical load, which does not represent actual physiological loading.

Wear simulation of hard-on-hard bearing surfaces has not been well studied. As the bearing materials are hard in nature, it has been assumed that the contact stress at the articulating surface is generally higher with the same geometry under the same physiological loading. However, the wear mechanism and progression on hard-on-hard bearing couples is actually different from that of a hard-on-soft couple. As a preclinical evaluation and design analysis, it would be important to understand and predict the contact stresses and the associated wear of such hard-on-hard bearing couples. Recently, by combining an analytical model based on the Hertz theory and an FE wear model based on the Reye hypotheses under a one-dimensional (1D) gait load, Cosmi et al. [17] qualitatively investigated the wear in Durom™ and Metasul™ hip joints (Co–Cr–Mo and Co–Cr–Mo). Similarly, Liu et al. [18] and Harun et al. [19] also studied the wear of the Co–Cr–Mo on Co–Cr–Mo hip resurfacing prostheses using the 1D gait load under a simplified gait motion of walking. A comprehensive understanding of the wear of hard-on-hard hip joint prostheses under truly 3D loading and gait motion cycles are not available. This potentially limits the optimization of this promising class of prostheses.

This paper aims to obtain an in-depth understanding of the wear of hard-on-hard bearing couples (PCD-on-PCD, ceramic-on-ceramic and metal-on-metal of total hip replacements). The finite element hip model to be established and investigated in this paper will consider a complete 3D physiological gait loading and kinematic motions of normal walking. The bearing surface wear will be incorporated into the finite element analysis by element re-meshing in accordance with gait cycles. To reflect the lubrication and roughness of the surface with the progress of wear, friction at the bearing interface will also be considered.

2. Materials and methods

2.1. Gait cycle

To mimic walking, the most common activity of a human body, a 3D physiological loading gait cycle was considered in the present analysis. Fig. 1 shows the axial components of the hip load and angle in a gait cycle of the left hip obtained from experimental analysis, where the gait cycle for different patients with total hip anthroplasty was described by 200 time instances [20]. The hip gait load and angle considered in this study are the average of several trials during normal walking activities of four patients. The angles are estimated based on the rotation of the hip

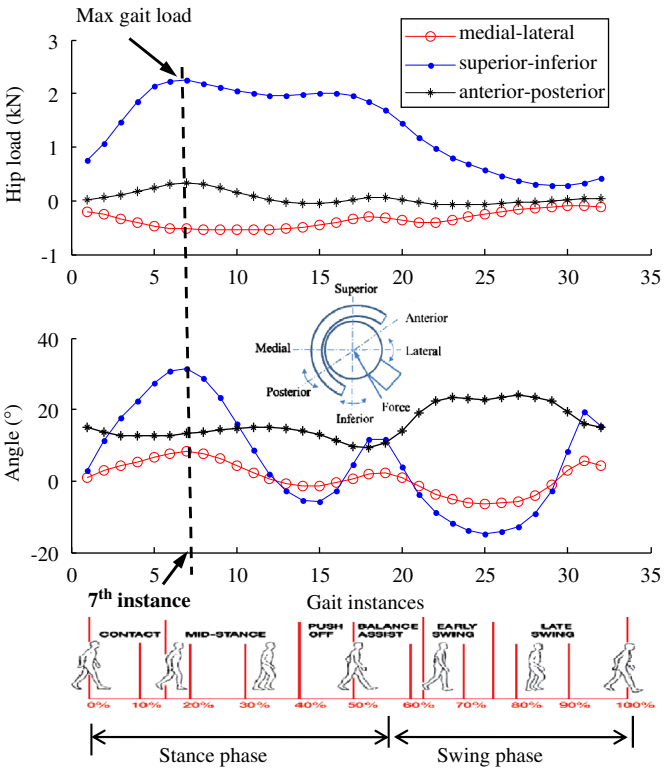

Fig. 1. Gait load and angle of a normal walking cycle [20].

stem about the medial–lateral, the anterior–posterior, and the superior–inferior axes, respectively (see Fig. 1). For the ease of computation, we divided the whole gait cycle into 32 discrete instances. The instances 1 to 19 are called the stance phase (the first 60% of the cycle) whereas instances 20–32 are called the swing phase (the rest 40% of the gait cycle). It is seen that the magnitude and direction of the load acting on the hip joint changes with the gait instances, and the maximum hip load of 2326 N appears at the 7th gait instance in the stance phase, which is approximately 2.5–3 times the average human body weight.

2.2. Wear model

According to the Archard's wear model (i.e., the abrasive–adhesive wear) [21], the sliding wear development on the articulating surfaces can be described by

$$W_V = K_w F S \tag{1}$$

where W_V denotes the volumetric wear of the bearing surface, K_w is the wear coefficient which can be obtained from experiment (e.g., pin-on-disc or hip wear simulator), F is the applied contact load, and S is the sliding distance between contacting surfaces. To calculate the linear wear on the surface, W_L, Eq. (1) can be modified by dividing both sides by an area as:

$$W_L = K_w P S \tag{2}$$

where P represents the contact stress.

Further, by discretising the whole gait cycle into certain instances or time intervals, the linear wear at any point on the surface for the gait cycle can be derived by modifying Eq. (2) as:

$$W_L = \sum K_w P_i S_i (i = 1,\ldots,n) \tag{3}$$

where, n denotes the total number of the instances or time intervals in the gait cycle, P_i and S_i represent the contact stress and sliding distance at the ith discrete instance, respectively.

By substituting the contact stress obtained from the finite element analysis into Eq. (3), the linear wear at the nodes of the bearing surface can be determined.

2.3. Finite element modeling

In order to minimize the computational complexity, let us consider only the key bearing components in a hip joint prosthesis, i.e., the femoral head and the acetabular cup. The finite element model was therefore constructed with a dense and homogeneous meshing of hexagonal solid elements (Solid 186, 187) using a commercially available FE code, ANSYS. Mesh convergence tests were performed, considering the possible variation of the material properties of the head and cup (i.e., PCD-on-PCD, ceramic-on-ceramic and metal-on-metal) to achieve an optimised meshing by minimising the effect of mesh size on the maximum contact stress (variation less than 2%). This gave rise to the total number of elements and nodes of 67,696 and 15,614, respectively, where the size of each element was about 1 mm. The 4212 contact elements at the head-cup interface were CONTA 174 and TARGE 170 which are 8-noded elements commonly used to represent contact between two 3D-surfaces and are found to support a relatively large deformation with a significant amount of sliding and friction efficiently. The convergence tests also showed that the maxima of the contact stress occurs at the same location of the bearing surface, indicating that the finite element model established could sufficiently accurately mimic the process.

As the main objective of this study is to investigate the wear of hard bearing couples, the geometrical parameters were selected as follows: radius of the femoral head = 14 mm, radial clearance = 50 μm and thickness of cup = 5 mm, because these values are common for a hard-on-hard bearing couple [22,23]. Fig. 2 shows the configuration of the 3D finite element model and its anatomical coordinate system. The cup is positioned with an anterior–posterior angle of 0° and an inclination (i.e., abduction–adduction) angle of 45° which is approximately the neutral position of the cup in the pelvic bone. The femoral head is positioned concentrically without any micro-separation with respect to the cup. As the contact stress at the bearing surface is required for wear analysis, only half of the femoral head without the stem section was considered. It has been reported [24] that including the pelvic bone in the model or not does would have negligible influence on the contact stress. Thus the model of this study does not consider the interface between the pelvic bone and the acetabular cup to further minimize the computation time.

A non-linear contact algorithm was used to solve the contact problem at the interface between the head and the cup. In a static or quasi-static analysis, the contact stress at the bearing interface is not significantly affected by the friction due to small relative tangential movements between the head and cup [25]. In walking cycles, due to the relative sliding under high contact stresses, wear is strongly influenced by the interface friction [26]. However, the frictional coefficient at the bearing interface varies with bearing materials. For example, Bergmann et al. [20] reported that the friction coefficient was between 0.1 and 0.2 for metal-on-metal couples, and Scholes et al. [27] claimed 0.16 for metal-on-metal while testing in bovine serum or fluid lubrication. Hall and Unsworth [28], however, reported that the coefficient was between 0.2 and 0.25 for metallic couples tested in bovine serum. For ceramic-on-ceramic and PCD-on-PCD bearing couples of hip implants, the friction coefficient was reported to be in a quite different regime. To calculate the frictional heating in a ceramic-on-ceramic couple, Fialho et al. [29] used a friction coefficient of 0.05 at the bearing interface. Feng and Field [30] reported that the diamond-on-diamond friction coefficient in an environment close to the lubrication by the fluid of human body was around 0.05. In the present study, therefore, the bearing surface friction coefficient will be taken as 0.2 for a metal-on-metal couple, and 0.1 for ceramic-on-ceramic and PCD-on-PCD couples.

The materials for the femoral head and the acetabular cup for all the bearing couples are linearly elastic. Their Young's moduli (E) and Poisson's ratios (υ) are listed in Table 1. The metallic couple is made of wrought Co–Cr–Mo alloy, a biomedical grade type (ASTM F75) while the ceramic couple is an alumina (Al_2O_3) based bio-ceramic. The nodes at the outer boundary surface of the cup are fixed (i.e., displacements of the nodes on the surface in X, Y, and Z directions are set to zero) while the 3D physiological loads at the 32 discrete instances corresponding to motions for flexion–extension (FE), abduction–adduction (AA), and inward–outward rotations (IER) at each gait instance (see Fig. 2) are applied through the centre node of the femoral head.

2.4. Updating the wear and geometry

To calculate the wear at the bearing surface in gait cycles, Eq. (3) is used with the contact stresses obtained from the finite element analysis. The sliding distance is obtained from the 3D hip gait motions, where a transformation matrix is determined by

Table 1
Material properties of bearing couples used in the computational analysis.

Bearing material	Young's modulus, E (GPa)	Poisson's ratio, υ
PCD	900	0.1
Al_2O_3	375	0.3
Co–Cr–Mo alloy	210	0.3

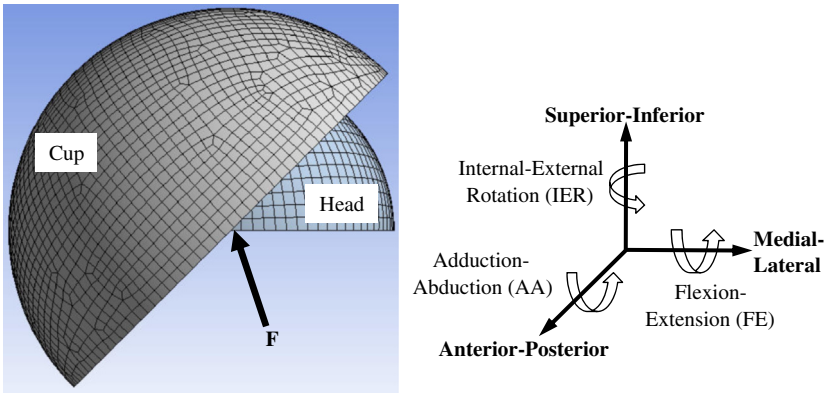

Fig. 2. The 3D finite element model and the coordinate system.

considering the Euler sequence of FE→AA→IER motions. Based on the linear wear computed, the volumetric wear of the surface becomes, according to Eq. (1),

$$W_v = \sum W_{Li} A_i (i = 1, \ldots, n) \quad (4)$$

where W_{Li} denotes the linear wear estimated at the finite element node i, which is the average of the four integration points of the ith element; A_i represents the area of the ith element, and n is the total number of elements in the worn region of the contacting surface. A femoral head surface normally wears equally to the cup surface. Thus in this study, the head wear analysis was not repeated.

Wear changes the geometry of a bearing surface, and hence the contact stresses. To take this effect into account, in this analysis, the geometry of a worn surface was updated by moving its nodes inward in the radial direction by an amount equal to the wear depth, and the surface with the modified geometry was re-meshed. Considering that a hip joint implant in a patient under normal routine activities experiences 1×10^6 cycles each year in average, the wear simulation in this study was carried out up to 2×10^6 cycles (equivalent to 2 years of hip joint motion). Thus the above geometry update was done at every 0.2×10^6 cycles, which was found to be sufficient to accurately count for the wear-induced contact stress changes. The wear coefficient, K_w, in Eq. (3) for the bearing couples was obtained either from hip simulator or pin-on-disc tests as listed in Table 2. For PCD and ceramic couples, the values of K_w were kept constant throughout the wear simulation. For the metal-on-metal couple, K_w needs to properly reflect the two phases of wear, the running-in and steady wear. Thus the values of K_w were based on relevant hip simulator studies [31]. It is worthwhile clarifying that during wear simulation, the bearing surface geometry update for the running-in phase was carried out only until 1×10^6 cycles (equivalent to 1 year).

Table 2
Wear coefficients.

Bearing couple	Wear coefficient, K_w (mm^3/N/m)
PCD-on-PCD	0.00459×10^{-8} [32]
Ceramic(Al_2O_3)-on-ceramic(Al_2O_3)	0.2×10^{-8} [8]
Metal(Co–Cr–Mo)-on-metal(Co–Cr–Mo)	0.5×10^{-8} (running-in) [31] 0.15×10^{-8} (steady state) [31]

3. Results and discussion

3.1. Contact stress

The contact stresses on the unworn bearing surfaces with respect to different instances of the gait cycles on all the three hard-on-hard couples first have been thoroughly studied. As their variations with gait instances are similar to each other, only the results of the PCD-on-PCD bearing couple are discussed in detail below.

Fig. 3 shows the contact stress distribution on the bearing surface at some selected gait instances. It is seen that due to the gait motion, the magnitude and location of the maximum contact stress change with the gait instance, with the highest (160.62 MPa) at the 7th gait instance in the stance phase corresponding to the peak gait load and the lowest (70.08 MPa) at the 29th gait instance in the swing phase of the cycle. With the given cup orientation at an inclination angle of 45°, the contact is always around the pole and within the bearing surface of the cup. This indicates that no edge contact occurs. However, with a steep cup inclination (i.e., larger than 45°) and under abnormal gait loading due to an unexpected activity, edge contact may take place, causing strip wear or breakage at the rim of the cup [22]. This further may cause dislocations of the head relative to the cup.

As PCD is hard and brittle, the variation of principal stresses is of primary importance. Fig. 4 shows that the dominant is the compressive minimum principal stress over the center of the contact zone. Similar to the maximum contact pressure distribution, the highest and lowest minimum principal stresses (−121.25 MPa and −45 MPa) occur when the hip gait motion reaches the 7th and 29th

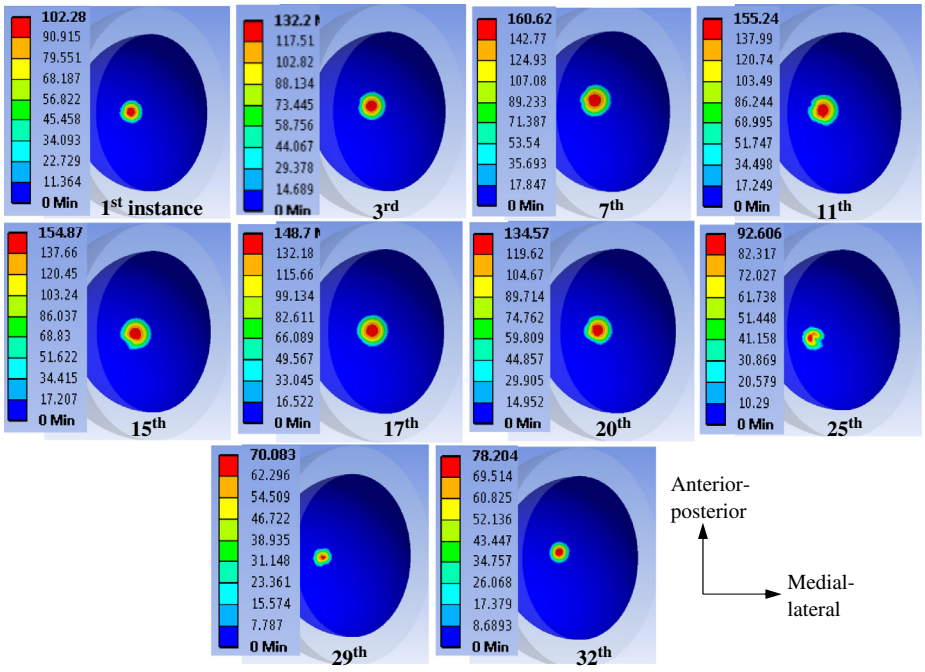

Fig. 3. The contact stress (MPa) distribution on the cup surface of the PCD-on-PCD bearing couple at selected gait instances.

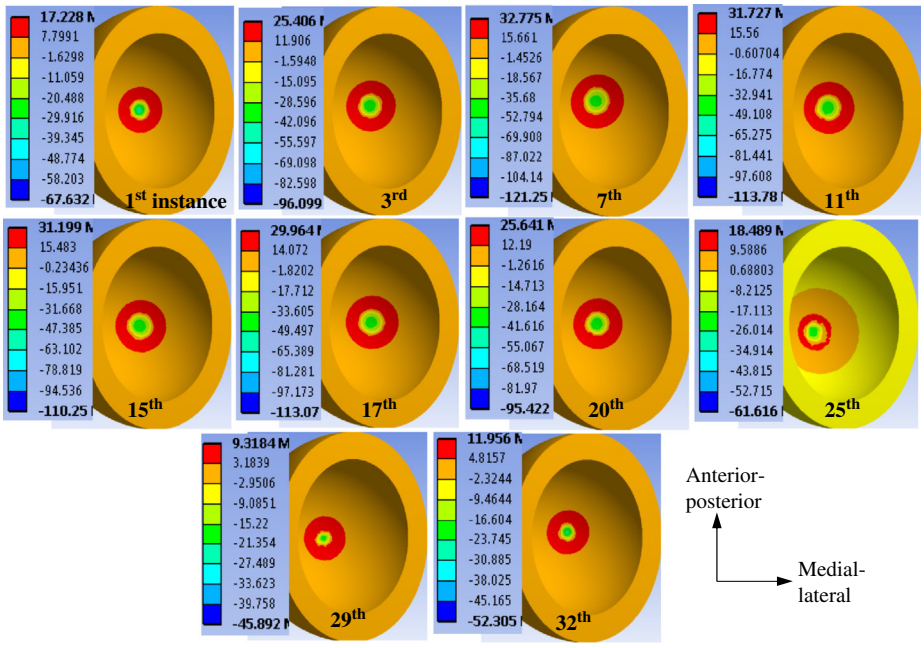

Fig. 4. The principal stress (MPa) distribution on the cup surface of the PCD-on-PCD bearing couple at some selected gait instances.

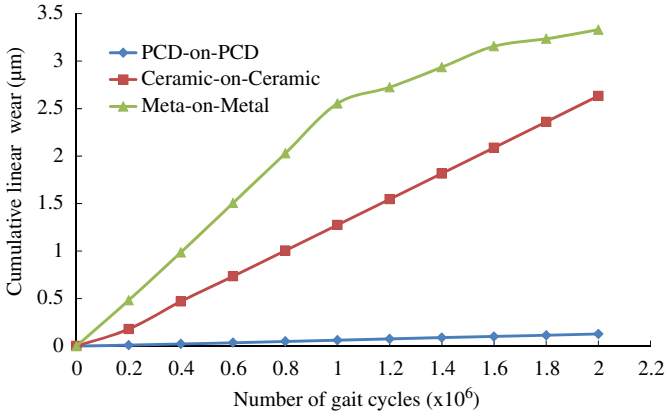

Fig. 5. Cumulative linear wear on the cup with gait cycles.

gait instances, respectively. As expected, compared to metal and ceramic couples, the contact pressure and stress are the highest in the PCD bearing couple, because PCD is the hardest. Further, for the given geometry of the joints in this study, the stress values are smaller than the yield strengths of the materials. This implies that stress induced by regular gait loading on the hard-on-hard bearing surface with no wear is less likely to cause severe damage. However this may not be the case when the bearing surface changes due to continuous wear. With the developed FE model, the current study thus aims to estimate wear generation and its evolution on the bearing surface, which are depicted in the following section.

3.2. Wear

3.2.1. Linear wear

Fig. 5 shows the cumulative linear wear on the cup surface with respect to the number of the gait cycles for all the three bearing couples. Compared to metal-on-metal and ceramic-on-ceramic, PCD-on-PCD bearing couple shows the least wear progression as the number of gait cycles increases. This is due to the smaller wear coefficient of the PCD couple. Table 3 lists the predicted overall wear evolution on the bearing couples. As can

Table 3
Predicted overall wear evolution on the bearing couples after 2×10^6 gait cycles.

Bearing couple	Linear wear (μm/year)	Volumetric wear (mm^3/year)
PCD-on-PCD	0.0635	0.00292
Ceramic-on-ceramic	1.317	0.17275
Co–Cr–Mo alloy-on-Co–Cr–Mo alloy	1.725	0.1425

be seen, the linear wear rate of the PCD couple was 0.06385 μm/(1×10^6 cycles) after 2×10^6 cycles, which is about only 5% and 4% of the wear rates of the ceramic and metal couples, respectively. The model predictions are in good agreement with the clinical and laboratory data available. For example, the predicted linear wear rate of the ceramic couple was 1.317 μm/(1×10^6 cycles), which is close to the record of 2–5 μm/(1×10^6 cycles) [33,34] in clinical studies. For metal-on-metal couple as shown in Fig. 5, there is a sharp increase in wear up to 1×10^6 cycles. This is because the wear coefficient in the phase of running-in wear is relatively high. The linear wear rate in the first million cycles is 2.5 μm/(1×10^6 cycles), but decreases to 0.95 μm/(1×10^6 cycles) in the second million cycles. Again, the above model prediction on the metal couple is in good agreement with measurement by clinical and/or laboratory studies (2.9–12.8 μm [35] and 1.27–15.7 μm [36] in the first million cycles).

It is to be noted that the estimated linear wear rate is lower than that of clinical/hip simulator tests. This may account for the use of wear coefficient that is within its lower end estimated from hip simulator or pin-on-disc tests [8]. Wear measurement errors when using CMM and laser scanning techniques may overestimate clinical/hip simulator value. For instance, during CMM measurement, the linear wear is measured as the maximum linear deviation between unworn rough surface and worn surface while the current simulation estimates linear wear considering the initial surface is smooth. Given these facts, it is imperative that the wear modelling developed in this study can reasonably simulate the linear wear progression of hip joint prostheses. In addition, the wear rates obtained from clinical and hip simulator tests vary in a very wide range due to many other uncertain

factors, which has significantly hindered a deep understanding of the wear mechanisms. Moreover, the model prediction has, to some extent, overcome such uncertainty.

3.2.2. Volumetric wear

Fig. 6 shows that the cumulative volumetric wear varies in a similar way to the linear wear. Because of the high wear resistance (low wear coefficients) of PCD, the PCD-on-PCD couple shows the lowest wear progression. Its overall volumetric wear rate was 0.00292 $mm^3/(1\times10^6$ cycles) in the first 2 million cycles, which is only 2% and 1% of the ceramic and metal couples, respectively (see also Table 3). Again, the above model prediction aligns well with the experimental measurement of 0.0036 $mm^3/(1\times10^6$ cycles) [32].

The volumetric wear rate for the ceramic couple is estimated to be 0.17275 $mm^3/(1\times10^6$ cycles). Hip simulator studies showed two different ranges of volumetric wear rate for the ceramic couples. Essner et al. [8], Clarke et al. [37], and Nevelos et al. [38] reported a lower volumetric wear rate of about 0.014–0.05 $mm^3/(1\times10^6$ cycles) while other studies measured relatively higher volumetric wear rate of about 0.10–1.015 $mm^3/(1\times10^6$ cycles) [9,39]. A volumetric wear rate on the retrieved ceramic implants is measured to be 1 $mm^3/(1\times10^6$ cycles) [39].

For the metal couple, the volumetric wear rate for the first year is 0.42 $mm^3/(1\times10^6$ cycles), and then decreases to 0.13 $mm^3/(1\times10^6$ cycles) up to second year. These results are consistent with hip simulator study, in which, the wear rate for the first year was 0.22 $mm^3/(1\times10^6$ cycles) and for the rest, 0.065 $mm^3/(1\times10^6$ cycles) [31]. By carrying out clinical tests on the retrieved implants, a relatively larger mean volumetric wear rate of about 0.545–3.74 $mm^3/(1\times10^6$ cycles) was reported elsewhere [35]. While the volumetric wear rate in literature is significantly scattered, the estimated volumetric wear rate lies within a zone between lower and higher range of clinical/hip simulator studies. The discrepancy may account for wide variety of important factors including wear test setup, test protocol, loading, and wear measuring technique used in both hip simulator and clinical studies across literature. For example, in laboratory environments, CMM, gravimetric, and fluid displacement methods are frequently adopted to measure wear volume [40] while radiographic imaging technique along with computational processing is used in clinical studies [41]. Inherent nature of these techniques may significantly affect wear volume measurements, hence resulting in such unexpected variation.

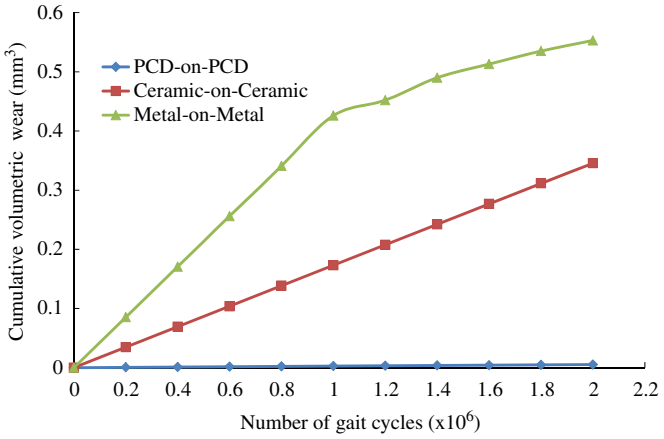

Fig. 6. Cumulative volumetric wear on the cup with gait cycles.

3.2.3. Wear scar and contact pressure

Fig. 7 illustrates the linear wear distribution on the cup surface for all three bearing couples after wear simulation up to 2×10^6 cycles. Compared to the ceramic and metal couples, worn area of the PCD couple is small in size. The simulated worn areas appear to be approximately circular in shape and are always located away from the pole of the cup surface in the medial direction. This is due to hip kinematics and directions of the physiological loading considered in this study. Similar wear patterns on the

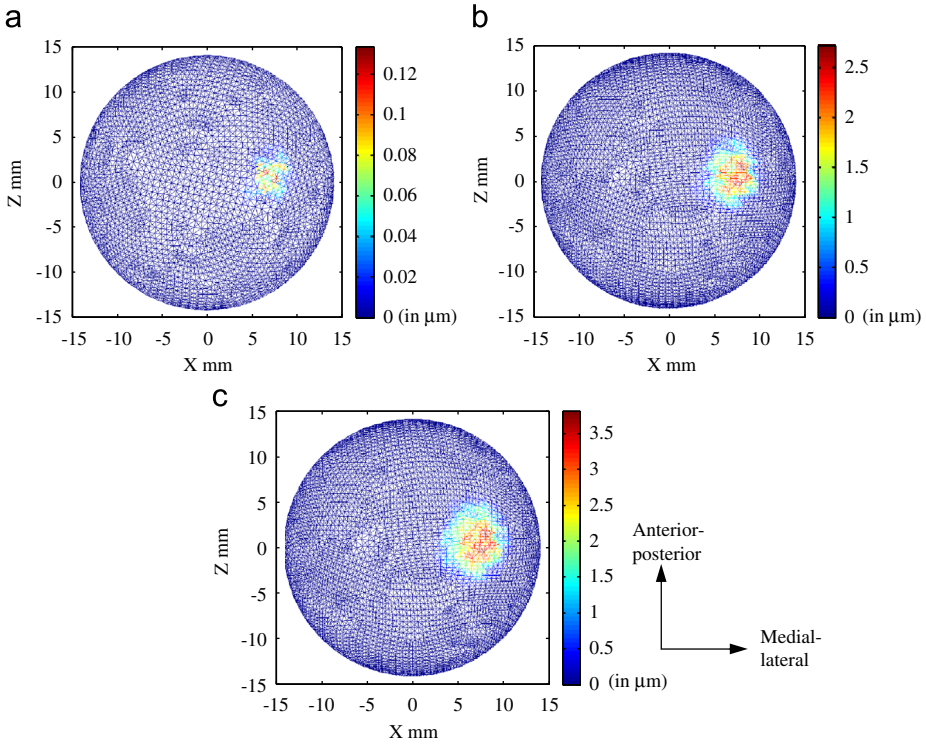

Fig. 7. Linear wear (µm) distribution on the cup surface for (a) PCD-on-PCD (b) ceramic-on-ceramic (c) metal-on-metal bearing couple after 2×10^6 cycles.

hard-on-hard bearing couples, mainly, for metal one, are observed by clinical and hip simulator observations [18]. The colour map (to the right side of the plots in Fig. 7) indicates the intensity of linear wear (in μm) on the surface. The maximum wear (i.e., wear depth) is not always located at the centre of worn region but being scattered within the region. The maximum linear wear for PCD, ceramic, and metal couples up to 2×10^6 cycles is estimated to be 0.14044 μm, 2.634 μm, and 3.331 μm, respectively. No wear marks are observed on the edge or rim of the cup. This is because the current FE contact model considers an ideal gait loading. In practice, wear on or near the edge of the cup surface may occur because of high stress concentration under an edge loading due to micro-separation and steep inclination of the cup relative to the head [22,42,43].

Fig. 8 depicts the contact pressure distribution on the cup surface at 7th instance (where maximum gait load occurs) for three bearing couples after 2×10^6 cycles. It is clearly seen that as the number of gait cycles continues to increase, the contact pressure distribution becomes scattered due to the effect of localized wear on the surface. This is quite analogous to linear wear patterns shown in Fig. 7, which supports the prediction accuracy of the current computational wear modelling. The maximum contact pressure becomes higher than that of initial cycle where the contact pressure is smoothly distributed over the surface (for instance, see Fig. 3). For example, after 2×10^6 cycles, the maximum contact pressure for the PCD, ceramic, and metal couples increases from 160.62 MPa to 217.48 MPa, from 64.06 MPa to 108.26 MPa, and from 67.73 MPa to 78.56 MPa, respectively. However, it is hypothesized that, with further increase of gait cycles for long-term wear investigation, the maximum contact pressure is expected to decrease because the bearing surface will become more conforming and smooth due to continuous wear, resulting in a decreased radial clearance and hence, an increased contact area. This will eventually lead to a decrease of wear progression as is reported by Liu et al. [18]. According to tribological theory, this phenomenon may potentially enhance the lubrication at the interface of bearing surfaces. Joyce et al. [44] observed similar phenomenon of self-polishing on worn regions of retrieved metal-on-metal implants and an improvement in lubrication.

As extensively studied by researchers, wear is recognised as the main cause of implant failure. While laboratory and/or clinical studies are relatively complex and costly, and often offer short-term information, numerical modelling takes the role to evaluate wear in the design and manufacture of implants. Based on the results and discussion presented in earlier sections, it is clearly demonstrated that the current computational wear modelling is able to estimate wear generation on the hard bearing couples. The study shows that the PCD couple is estimated to generate the least wear over the ceramic and metal couples. This thus makes PCD an attractive material and potentially being used in the design of next generation's THR devices to alleviate concern over wear debris and ion release. It is worth noting that material properties, geometric characteristics, sliding distance need to be

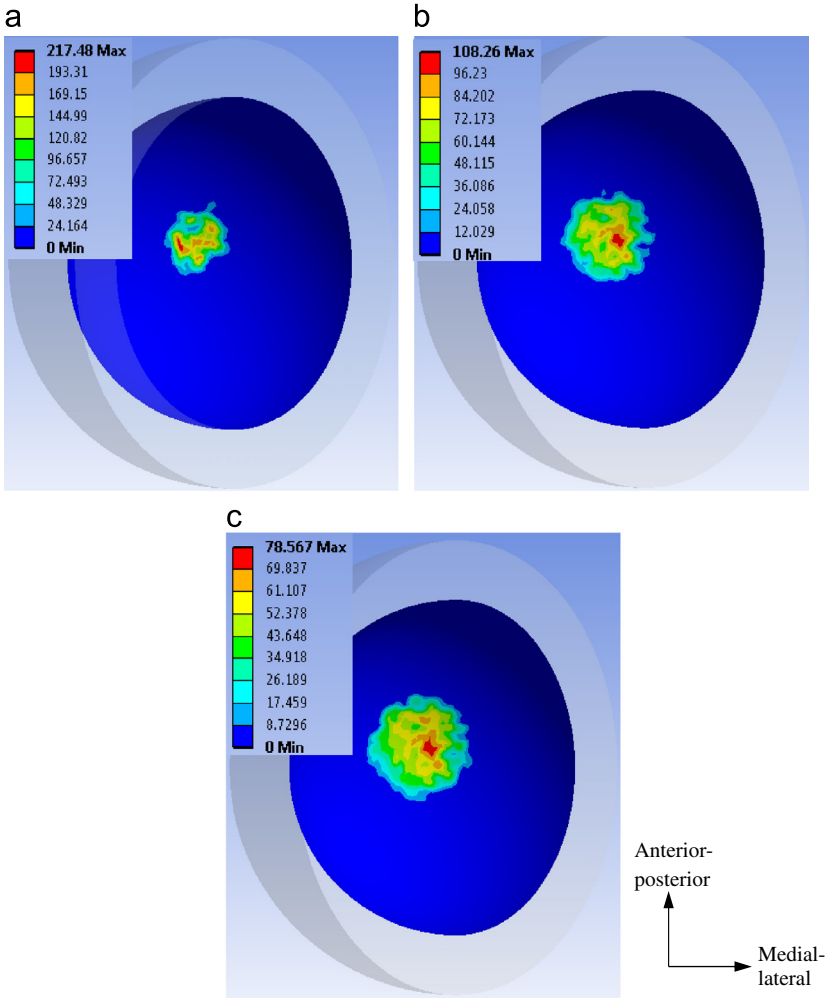

Fig. 8. Contact pressure (MPa) distribution on the cup surface at 7th instance (maximum load) of the gait after 2×10^6 cycles for (a) PCD-on-PCD (b) ceramic-on-ceramic (c) metal-on-metal bearing couples.

correctly adopted in wear modelling [45]. In this study, we stress the importance of 3D kinematics and gait motions to calculate sliding distance. For instance, Fialho et al. [29] indicated that 3D sliding distance increases about 18% volumetric wear when tested with a HSR patient as compared to a simplified two dimensional flexion–extension analysis. Another potential aspect with the hard bearing couples would be the temperature rise due to frictional sliding at the interface between the head and cup, which may affect material properties, friction [46]. Even though we considered a constant frictional coefficient to reflect a realistic surface condition at the interface, and showed seemingly reasonable wear generation, the temperature effect cannot be ignored in wear modelling when evaluating long-term wear performance of implants. We focused on updating surface geometry due to wear at a certain interval of gait cycles of $0.1–0.2 \times 10^6$ cycles. While these values are quite reasonable compared to other studies [15], a constant but small interval of gait cycles throughout simulation may mimic evolution of worn surface and hence ensure more accurate estimation of wear.

There are a number of limitations that may impede the performance of the present computational wear modelling. For instance, a constant wear coefficient value is used for the bearing couples throughout simulation. As wear progresses, however, the contact between the cup and the head changes continuously, and consequently, the lubrication at the interface [47]. The effect of lubrication on wear progression by changing wear coefficients is not considered explicitly. In addition, the current wear model was based on the abrasion-adhesion wear. To more accurately estimate the wear of hard-on-hard implants, other wear mechanisms, such as those due to surface fatigue and tribo-corrosion [48], will need to be incorporated. The hip loading adopted is based on the steady-state gait cycles, but *in-vivo* abnormal gait loading from wide range of activities may intensify stresses which may result in an increased wear. Further, the current wear simulation is limited up to 2×10^6 cycles (equivalent to 2 years of implant) which may not be sufficient to reflect actual wear evolution. As is widely reported, generally THRs in human body are expected to survive 15–20 years or more. It is thus important to study and evaluate wear progression for a longer period of time, which will enable us to predict more realistic behaviour of contact and wear of THRs. These will be addressed and incorporated in future studies.

4. Conclusions

This paper has carried out a comprehensive finite element analysis of the contact stress and wear in hard-on-hard hip joint prostheses under 3D physiological gait loading in walking cycles. The study concludes the following:

(1) Due to the gait motion, the intensity and location of the maximum contact stress in the bearing components change with the gait instances, with the highest at the 7th gait instance in the stance phase corresponding to the peak gait load, and the lowest at the 29th gait instance in the swing phase of the cycle.
(2) With the cup inclination angle investigated, i.e., 45°, it was found that the contact is always around the pole and within the bearing surface of the cup. It is reasonable to expect that under a steeper cup inclination (i.e., larger than 45°) and abnormal gait loading due to unexpected walking activities, edge contact may take place and in turn cause strip-wear/breakage at the rim of the cup and dislocations of the head relative to the cup.
(3) With a given geometry and gait loading, the linear and volumetric wear on the cup surface increases with the number of the gait cycles. The worn areas appear circular in shape and are always located away from the pole of the cup surface in the medial–lateral direction. With the increase of gait cycles, the contact pressure distribution will be scattered due to the effect of the localized wear on the surface.
(4) Compared to ceramic-on-ceramic and metal-on-metal, PCD-on-PCD bearing couple has the lowest wear progression in terms of cumulative linear and volumetric wear. This confirms the potential applicability of PCD couple in hip joint replacements.
(5) By comparing with the results of clinical and/or hip simulator studies, we found that the computational wear model presented in this paper can provide a reasonable estimation of the wear evolution in hard-on-hard hip implants.

Acknowledgements

The authors would like to thank the Australian Research Council (ARC) for its financial support to carry out the research presented in this paper.

References

[1] M. Kurth, P. Eyerer, R. Ascherl, K. Dittel, U. Holz, An evaluation of retrieved UHMWPE hip joint cups, Journal of Biomaterials Applications 3 (1) (1988) 33–51.
[2] W. Rieger, Ceramics in orthopaedics—30 years of evolution and experience, in: C. Reiker, S. Oberholzzer, and U. Wyss (Eds.), Proceedings of the World Tribology Forum on Anthroplasty, (Verlag Hans Huber, Bern), 2001, pp. 1–14.
[3] T. Visuri, E. Pukkala, Does metal-on-metal total hip prosthesis have influence on cancer? A long-term follow-up study, World Tribology Forum in Anthroplasty (2001) 181–188. (Hans Huber).
[4] I.C. Clarke, L. Anissan, A. Stark, A. Gustafson, V. Good, P. Williams, B. Downs, L. Yu, Comparison of M–M and M–PE hip systems at 10 million cycles in hip simulator study, in: Reiker, C., Windler, M., Wyss, U. (Eds.), Metasul–A Metal on Metal Bearing, (Hans Huber, Bern), 1999, pp. 93–108.
[5] B.J. Pope, J.K. Taylor, R.H. Dixon, C.F. Gardinier, L.M. Pope, D.C. Blackburn, M.A. Vail, K.M. Jensen, Prosthetic Hip Joint Having at Least One Sintered Polycrystalline Diamond Compact Articulation Surface and Substrate Surface Topological Features in Said Polycrystalline Diamond Compact, US Patent No: 6402787 B1, 2002.
[6] Y. Chen, L.C. Zhang, J. Arsecularatne, C. Montross, Polishing of polycrystalline diamond by the technique of dynamic friction, Part 1: Prediction of the interface temperature rise, International Journal of Machine Tools and Manufacture 46 (6) (2006) 580–587.
[7] H.P. Sieber, C.B. Rieker, P. Kottig, Analysis of 118 second generation metal-on-metal retrieved hip implants, Journal of Bone and Joint Surgery British 81 (1999) 46–50.
[8] A. Essner, K. Sutton, A. Wang, Hip simulator wear comparison of metal-on-metal, ceramic-on-ceramic and cross-linked UHMWPE bearings, Wear 259 (2005) 992–995.
[9] S. Affatato, G. Bersaglia, I. Foltran, D. Emiliani, F. Traina, A. Toni, The influence of implant position on the wear of alumina-on-alumina studied in a hip simulator, Wear (2004) 400–405.
[10] A.C. Cilingir, Finite element analysis of the contact mechanics of ceramic-on-ceramic hip prostheses, Journal of Bionic Engineering 7 (2010) 244–253.
[11] R.K. Korhonen, A. Koistinen, Y.T. Konttinen, S.S. Santavitra, R. Lappalainen, The effect of geometry and abduction angle on the stresses in cemented UHMWPE acetabular cups- finite element simulations and experimental test, BioMedical Engineering OnLine 4 (32) (2005).
[12] T.A. Maxian, T.D. Brown, D.R. Pederson, J.J. Callaghan, Adaptive finite element modelling of long-term polyethylene wear in total hip anthroplasty, Journal of Orthopaedic Research 14 (41) (1996) 668–675.
[13] S.H. Teoh, W.H. Chan, R. Thampuran, An elasto-plastic finite element model for polyethylene wear in total hip anthroplasty, Journal of Biomechanics 35 (2002) 323–330.
[14] S.L. Bevil, G.R. Bevil, J.R. Penmetsa, A.J. Petrella, P.K. Rullkoetter, Finite element simulation of early creep and wear in total hip anthroplasty, Journal of Biomechanics 38 (2005) 2365–2374.
[15] G. Matsoukas, R. Willing, Y. Kim II, Total hip wear assessment: a comparison between computational and *in vitro* wear assessment techniques using ISO14242 loading and kinematics, Journal of Biomechanical Engineering 131 (2009) 1–11.
[16] L. Kang, A.L. Galvin, J. Fisher, Z. Jin, Enhanced computational prediction of polyethylene wear in hip joints by incorporating cross-shear and contact pressure in addition to load and sliding distance: effect of head diameter, Journal of Biomechanics 42 (2009) 912–918.

[17] F. Cosmi, M. Hoglievina, G. Fancellu, B. Martunelli, Finite element method comparison of wear in two metal-on-metal total hip prostheses, Journal of Engineering in Medicine 220 (2006) 871–879.
[18] F. Liu, I. Leslie, S. Williams, J. Fisher, Z. Jin, Development of computational wear simulation of metal-on-metal hip resurfacing replacements, Journal of Biomechanics 41 (2008) 686–694.
[19] M.N. Harun, F.C. Wang, Z.M. Jin, J. Fisher, Long-term contact-coupled wear prediction for metal-on-metal total hip joint replacement, Journal of Engineering Tribology 223 (2009) 993–1001.
[20] G. Bergmann, G. Deuretzbacher, M. Heller, F. Graichen, A. Rohlmann, J. Strauss, G.N. Duda, Hip contact forces and gait patterns from routine activities, Journal of Biomechanics 34 (2001) 639–642.
[21] J.F. Archard, Contact and rubbing of flat surfaces, Journal of Applied Physiology 24 (1953) 981–988.
[22] M.M. Mak, A.A. Besong, Z.M. Jin, J. Fisher, Effect of micro-separation on contact mechanics in ceramic-on-ceramic hip joint replacements, Journal of Engineering in Medicine 216 (2002) 403–408.
[23] M.M. Mak, Z.M. Jin, Effect of acetabular cup position on the contact mechanics of ceramic-on-ceramic hip joint replacements, Key Engineering Materials 254-256 (2004) 639–642.
[24] S. Barreto, J. Folgado, P.R. Fernandes, J. Monteiro, The influence of the pelvic bone on the computational results of the acetabular component of a total hip prosthesis, Transactions of the ASME-Journal of Biomechanical Engineering 132 (5) (2010) 054503 1-4.
[25] M.S. Uddin, L.C. Zhang, Contact stresses of PCD-on-PCD hip joint prostheses, in: Proceedings of Seventh International Conference on Advances and Trends in Engineering Materials and Their Applications, July 4–8, Milan, Italy, 2011, pp. 135–143.
[26] F.C. Wang, C. Brockett, S. Williams, I. Udofia, J. Fisher, Z.M. Jin, Lubrication and friction prediction in metal-on-metal hip implants, Physics in Medicine and Biology 53 (2008) 1277–1293.
[27] S.C. Scholes, S.M. Green, A. Unsworth, The wear of metal-on-metal total hip prostheses measured in hip simulator, Journal of Engineering in Medicine 215 (2000) 523–530.
[28] R.M. Hall, A. Unsworth, Friction in hip prostheses, Biomaterials 18 (1997) 1017–1026.
[29] J.C. Fialho, P.R. Fernandes, L. Eca, J. Folgado, Computational hip joint simulator for wear and heat generation, Journal of Biomechanics 40 (2007) 2358–2366.
[30] Z. Feng, J.E. Field, The friction and wear of diamond sliding on diamond, Journal of Physics D: Applied Physics 25 (1992) A33–A37.
[31] F.W. Chan, J.D. Bobyn, N.B. Medley, J.J. Krygeir, M. Tanzer, The Otto Aufranc Award—wear and lubrication of metal-on-metal hip implants, Clinical Orthopaedics and Related Research 369 (1999) 10–24.
[32] D. Harding, D. Blackburn, G. Loesener, R. Dixon, B.K. Nguyen, Wear rate comparison between polycrystalline diamond, CoCr, and UHMWPE in high wear environments, in: International Society for Advanced Spine Surgery (ISASS) Conference, 28–29 April, 2011, Nevada, USA.
[33] J.M. Dorlot, Long-term effects of alumina components in total hip prostheses, Clinical Orthopaedics and Related Research 282 (1992) 47–52.
[34] H. Mittelmeier, J. Heisel, Sixteen year's experience with ceramic hip prostheses, Clinical Orthopaedics and Related Research 282 (1992) 64–72.
[35] G. Reinisch, K.P. Judmann, C. Lhotka, F. Lintener, K.A. Zweymuller, Retrieved study of uncemented metal-on-metal hip prostheses revised for early loosening, Biomaterials 24 (2003) 1081–1091.
[36] J.B. Medley, F.W. Chan, J.J. Krygier, J.D. Bobyn, Comparison of alloys and designs in a hip simulator study of metal on metal implants, Clinical Orthopaedics and Related Research 329 (1996) S148–S149.
[37] I.C. Clarke, V. Good, P. Williams, D. Schroeder, L. Anissian, A. Stark, H. Oonishi, J. Schuldies, G. Gustafson, Ultra-low wear rates of rigid-on-rigid bearings in total hip replacements, Journal of Engineering in Medicine 214 (2000) 331–347.
[38] J.E. Nevelos, E. Ingham, C. Doyle, A.B. Nevelos, J. Fisher, The influence of acetabular cup angle on the wear of BIOLOX Forte alumina ceramic bearing couples in a hip simulator, Journal of Materials Science Materials in Medicine 12 (2001) 141–144.
[39] T. Stewart, J. Nevelos, J. Tipper, G. Insley, R. Streicher, E. Ingham, J. Fisher, Long Term Simulator Studies of Alumina Ceramic/Ceramic Hip Joints with Swing Phase Micro-separation; Analysis of Wear and Wear Debris Generation.
[40] T. Mizoue, K. Yamamoto, T. Masaoka, A. Imakiire, M. Akagi, Validation of acetabular cup wear volume based on direct and two dimensional measurements: hip simulator analysis, Journal of Orthopaedic Science 8 (2003) 491–499.
[41] E. Ebramzadeh, S.N. Sangiorgio, F. Lattuada, J.S. Kang, R. Chiesa, H.A. Mckellop, L.D. Dorr, Accuracy of measurement of polyethylene wear with use of radiographs of total hip replacements, The Journal of Bone and Joint Surgery, Inc. (2003) 2378–2384.
[42] P.J. Lusty, W.L. Walter, Minimizing squeaking and edge loading when implanting a ceramic-on-ceramic hip anthroplasty, European Muscular Review (2007) 73–75.
[43] J.M. Elkins, K.M. Kruger, D.R. Pedersen, J.J. Callaghan, T.D. Brown, Edge loading severity as function of cup lip radius in metal-on-metal total hips—a finite element analysis, Journal of Orthopaedic Research (2011) 1–9.
[44] T.J. Joyce, H. Grigg, D.J. Langton, A.V.F. Nargol, Quantification of self-polishing *in vivo* from explanted metal-on-metal total hip replacements, Tribology International 44 (5) (2010) 513–516.
[45] O. Calonius, V. Saikko, Analysis of relative motion between femoral head and acetabular cup and advances in computation of the wear factor for prosthetic hip joint, Acta Polytechnica Scandinavica - Chemical Technology Series 3 (4) (2003) 43–54.
[46] J.W. Pritchett, Heat generated by hip resurfacing prostheses: an *in vivo* pilot study, Journal of Long-Term Effects of Medical Implants 21 (1) (2011) 55–62.
[47] D. Zhu, A. Martini A, W. Wang, Y. Hu, B. Lisowsky, Q. Wang, Simulation of sliding wear in mixed lubrication, Transactions of the ASME-Journal of Tribology 129 (2007) 544–550.
[48] M.A. Wimmer, J. Loos, R. Nassutt, M. Heitkemper, A. Fischer, The acting wear mechanisms on metal-on-metal hip joint bearing: *in vitro* results, Wear 250 (2001) 129–139.